

INTERNATIONAL SOCIETY FOR SOIL MECHANICS AND GEOTECHNICAL ENGINEERING



This paper was downloaded from the Online Library of the International Society for Soil Mechanics and Geotechnical Engineering (ISSMGE). The library is available here:

<https://www.issmge.org/publications/online-library>

This is an open-access database that archives thousands of papers published under the Auspices of the ISSMGE and maintained by the Innovation and Development Committee of ISSMGE.

Evaluation of three-dimensional tunnel face failure mechanism using X-ray CT

Evaluation des mécanismes d'effondrement tridimensionnels du front de taille d'un tunnel par auscultation par rayons X (X-ray CT)

J. Otani & D. Takano

Department of Civil and Environmental Engineering, Kumamoto University, Kumamoto 860-8555, Japan
 junotani@kumamoto-u.ac.jp

H. Nagatani

Geotechnical Engineering Group, Kajima Technical Research Institute, Tokyo 113-0032, Japan
 nagatanh@kajima.com

ABSTRACT

A tunnel face failure is simulated by pulling out a tunnel model set in a model ground. The ground is then investigated by X-ray computed tomography (CT) scanner in order to not only visualize the failure zone in three-dimension but also evaluate mechanism of the face failure. Here, the effect of overburden and pull-out length on the scale of failure zone is evaluated quantitatively. Finally, it is concluded that the mechanism of face failure can be investigated visually in three-dimension by the proposed test method. And the quantitative discussion on the face failure mechanism is well performed.

RÉSUMÉ

L'effondrement du front de taille d'un tunnel est étudié expérimentalement sur modèle réduit en simulant l'excavation progressive du sol du front de taille. Le sol est alors ausculté par rayon X grâce à un scanner, pour d'une part, visualiser la zone de rupture en trois dimensions, et pour d'autre part, évaluer le mécanisme d'effondrement. Ici, les effets de la profondeur d'enfouissement et de la quantité de matériau excavé sur les dimensions de la zone de rupture sont évalués quantitativement. Finalement, on en conclut que le mécanisme d'effondrement du front de taille du tunnel peut être obtenu visuellement en trois dimensions par la méthode proposée, et que quantitativement il est bien reproduit.

1 INTRODUCTION

In the mountain tunneling and shield tunneling methods, tunnel faces become very unstable due to stress release caused by excavation. When a face loses its stress balance, a slip surface occurs in the ground behind the face, leading to a local failure or a large-scale failure that extends up to the ground surface as shown in Fig. 1. Some information is needed to evaluate the stability of the face: i.e. the failure strength corresponding to the weight of the entire slide mass at the critical state of failure, resistance on the face, and shear resistance on the slip surface. In a typical design approach, face stability is evaluated based on the slip surface behind the face, which may be estimated by the logarithmic spiral method, and a loosen zone caused by arching effect above the slip surface. This approach evaluates the failure zone two-dimensionally, which is actually three-dimensional in shape. Because of the three-dimensional nature of shear resistance on the slip surface, the conventional approach may lead to overestimation of the failure strength of the face (Chambon et al., 1994; Mashimo et al., 1999; Konishi et al., 2000)

In the present study, a face failure is simulated by pulling out a tunnel model set in a model ground. The ground is then investigated by X-ray computed tomography (CT) to visualize the failure zone on a three-dimensional basis and elucidate the mechanism of face failure. Also, the effect of overburden and pull-out length on the failure zone is evaluated quantitatively.

2 OUTLINE OF TEST

2.1 Test setup

An industrial X-ray CT system was used in the present study (Otani et al., 2000; Otani et al., 2002a; Otani et al., 2002b). A model testing setup dedicated to X-ray CT is prerequisite for achieving sufficient precision in test results. The setup developed in this study for tunnel pull-out model testing using X-ray CT is shown in Fig. 2. The cylindrical soil tank has an outer

diameter of 150 mm and an inner diameter of 125 mm. The ground model can be as high as 300 mm. The tunnel model consists of a pipe, which has an outer diameter of 20 mm, and a pull-out core, which has an outer diameter of 13 mm. The center of the tunnel model is set at a height of 100 mm from the bottom of the cylindrical soil tank, with the tunnel model extruding 20 mm from the tank side. By sealing the top of the soil tank and placing a water bag on the ground surface, a surcharge by air pressure can be provided.

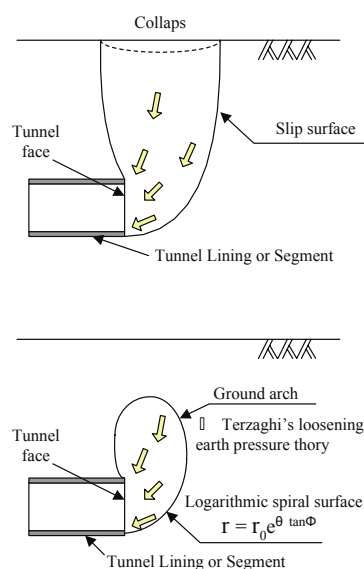


Figure 1. Tunnel face failure.

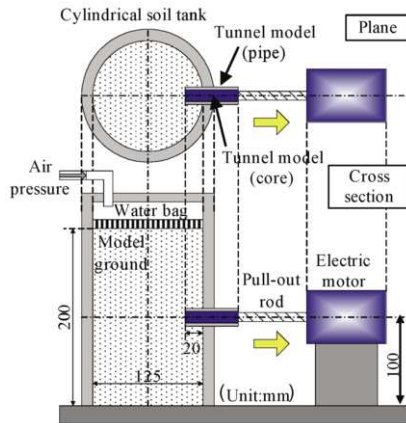


Figure 2. Tunnel pull-out model test system.

Table 1. Test cases.

Test case	Overburden ratio	Overburden depth	Pull-out length	Pull-out velocity	Remark
		mm	mm	mm/sec	
CASE1	4D	52	1	0.1	Critical state model
CASE2	4D	52	10	0.1	Large-scale failure model
CASE3	2D	26	1	0.1	Critical state model
CASE4	1D	13	1	0.1	(Effect of overburden)

1D:Outer diameter of tunnel core

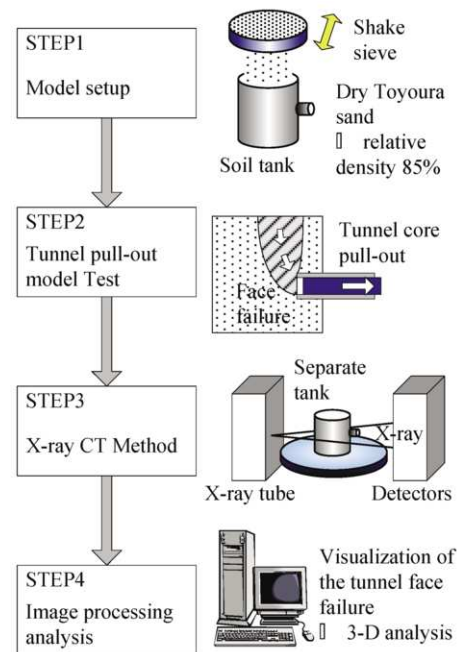


Figure 3. Experimental procedure.

2.2 Test method

The entire test procedure is shown in Fig. 3. Dry Toyoura sand was used as the ground model material, and a relative soil density of 85% was achieved by the free-fall method using multiple sieves. After preparing the soil in the cylindrical soil tank (STEP1), the tank was set in the tunnel pull-out model test system and the core part was pulled out by a certain length (STEP2). The tank was then removed and set on a turntable in an X-ray CT booth for investigation (STEP3). CT images were taken at a 1-mm pitch from the tunnel bottom to the soil surface. The cross-sectional images were subjected to simple local smoothing and layered to form three-dimensional images (STEP4). The CT images were processed by wire-framing to evaluate the generated soil failure quantitatively.

2.3 Test conditions

The cases and the conditions of the test are listed in Table 1. With the outer diameter of the pull-out core (13 mm) expressed as 1D, the conditions of the basic case (CASE 1) are an overburden of 4D, a pull-out length of 1 mm, and a pull-out rate of 0.1 mm/sec. A total of four different cases, including a pull-out length of 10 mm and overburdens of 1D, 2D, and 4D, were investigated. These test cases were specified by focusing on overburden and pull-out length, which are factors that influence the mechanism of face failure.

3 TEST RESULTS

3.1 Visualization of the mechanism of face failure

When confirming face stability by a tunnel pull-out model test, a typical practice is to simulate the critical state of face failure by pulling out the tunnel by about 10% of the face height. In the present test, therefore, the core part was pulled out by 1 mm to loosen the face and evaluate the critical state of failure (CASE1).

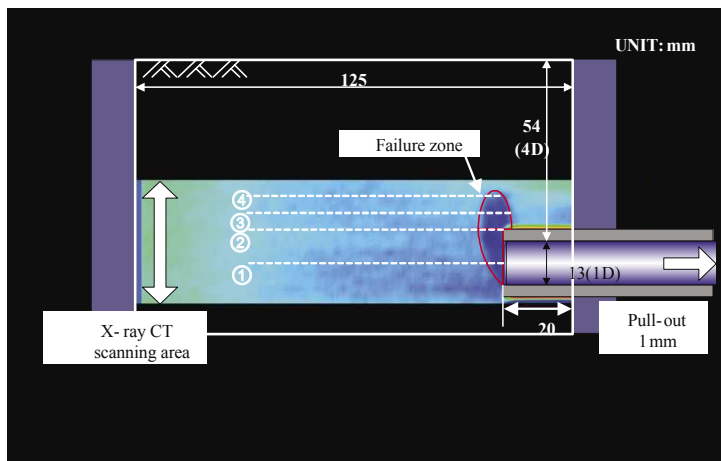
Here, overburden was set to 4D so that sufficient arching effect would occur in the soil at the time of face failure. Examples of CT images obtained for CASE 1 are shown in Fig. 4. The locations of the four horizontal-section images given in Fig. 4(b) are indicated in Fig. 4(a), which is a vertical-section image obtained by layering all the horizontal-section images. The horizontal-section images indicate that the semicircular slip line extending behind the face becomes elliptic above the level of tunnel crown and gets smaller upward. The vertical-section image indicates that a slightly arced slip line is developed behind the face and a failure zone (loosen zone) caused by arching effect, which is typically observed in trap door tests, is present above the level of tunnel roof. This corresponds to the failure zone described in Fig. 1, and the zone is well recognized three-dimensionally in the present test.

The mechanism of large-scale face failure is discussed next. A large-scale failure in the tunnel was modeled by increasing the pull-out length to 10 mm with an overburden of 4D (CASE2). Figure 5 shows CT images in the same manner as Fig. 4. In CASE 2, as seen from the vertical-section and three-dimensional images, the failure zone extends nearly up to the ground surface and is closed near the surface because of the arching effect. The horizontal-section images indicate that the failure zone near the tunnel crown is elliptic as is the case with the critical-state model with a pull-out length of 1 mm and that the zone extends upward while maintaining the elliptic cross-sectional shape.

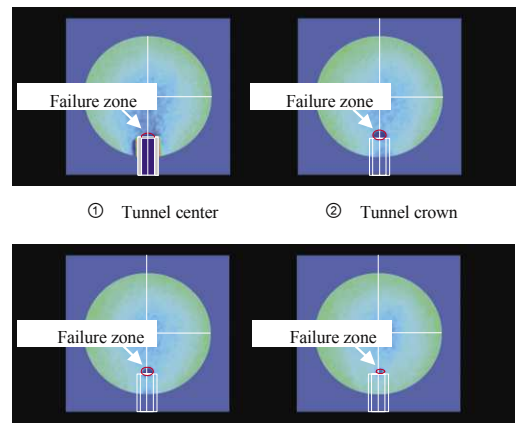
Based on the above test results, the slip surface behind the face and the failure zone extending upward are compared between the critical state and a large-scale failure state in Fig. 6, which shows three-dimensional wire-frame images. The slip surface generated behind the face does not change much between the critical and large-scale failure states. The failure zone, on the other hand, extends straightly upward from the critical to large-scale failure states.

3.2 Effect of overburden on arching

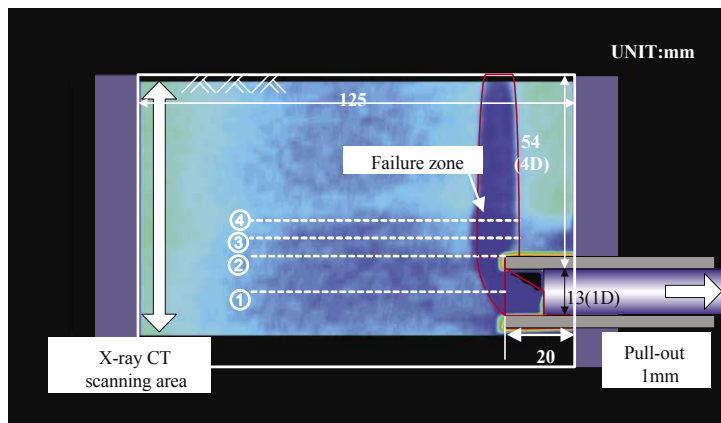
As shown by the X-ray CT images, a failure zone (loosen zone) is generated by arching effect when there is a sufficient over-



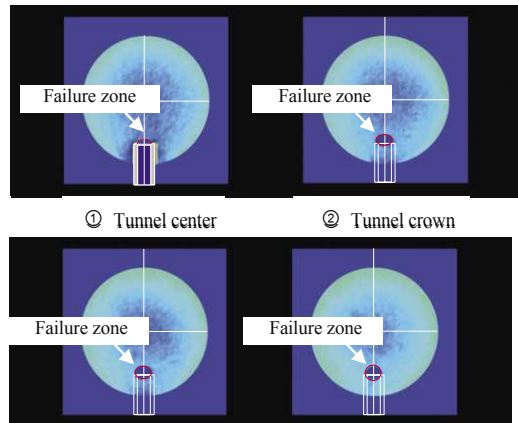
(a) Vertical-section image



③ 5 mm above the crown ④ 10 mm above the crown
(b) Horizontal-section images



(a) Vertical-section image



③ 5mm above the crown ④ 10mm above the crown
(b) Horizontal-section images

Figure 5. Cross sectional images (CASE2: Large-scale failure model).

burden at the time of face failure. Although depending on soil conditions, it is generally said that arching occurs when overburden exceeds 1D or 2D. The effect of overburden on arching is discussed here by comparing the failure zones corresponding to the overburdens of 1D, 2D, and 4D. Shown in Fig. 7 are three-dimensional wire-frame images depicting the failure zones of the three cases. Arching is not observed in the case of 1D because the failure zone extends straightly upward to the ground surface. However, the failure zone is closed in the cases of 2D and 4D because of arching effect. The slip surface generated behind the face is not affected by overburden.

Based on the above results, the volume of failure zone behind the face was calculated for each overburden, as plotted in Fig. 8. The volumes are nearly the same in 2D and 4D, but smaller in 1D because the failure zone reached the ground surface. As shown quantitatively in the present test, an overburden of 2D or more is sufficient to cause arching, and the shape of failure zone is not affected by overburden. It should be noted, however, that dry sand without viscosity was used in the model ground. A similar test using a cohesive soil material is therefore required to make a general discussion.

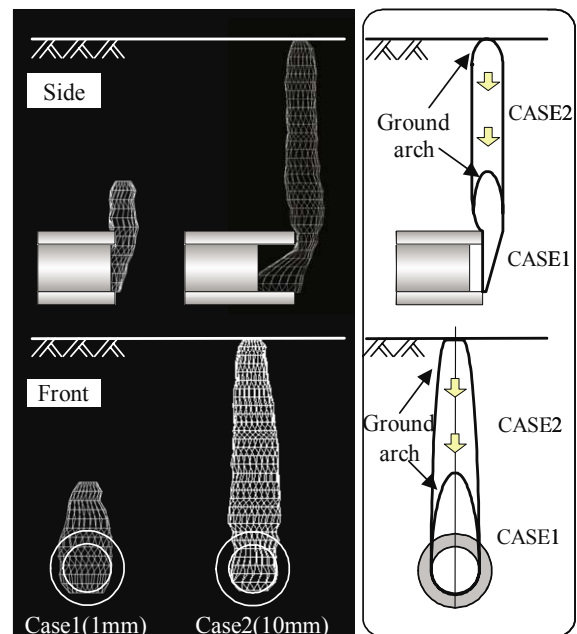


Figure 6. Comparison between CASE1 and CASE2.

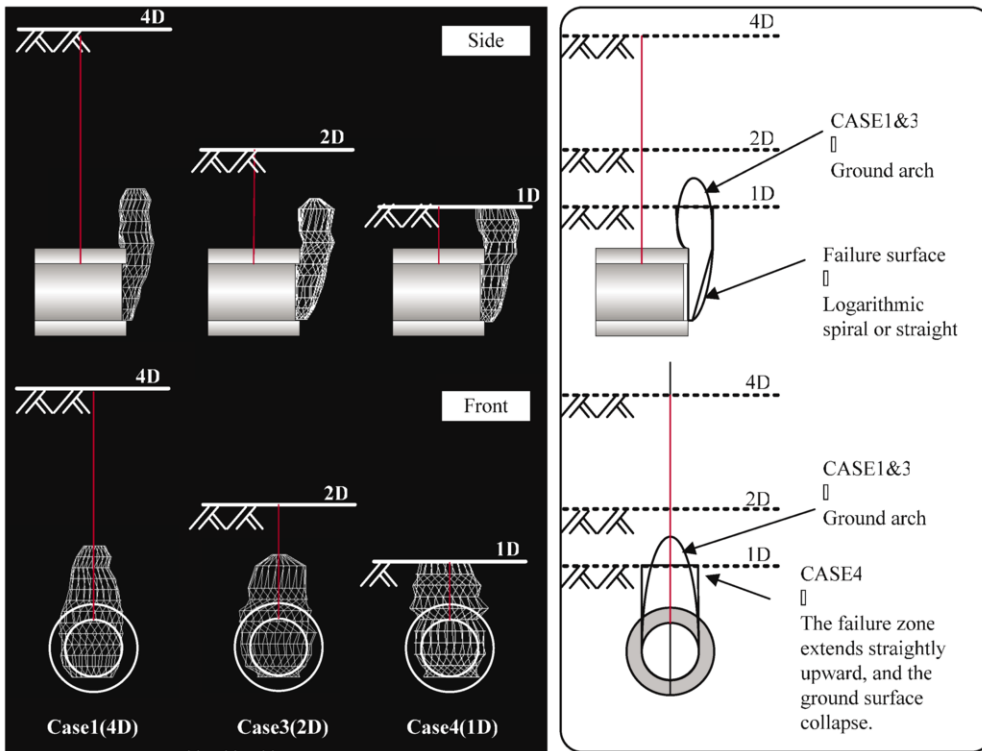


Figure 7. Comparison between CASE1, CASE3 and CASE4.

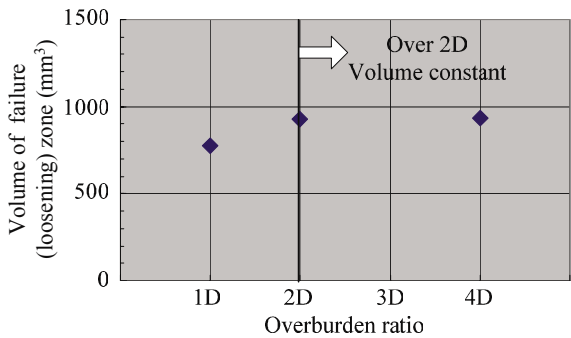


Figure 8. Volume of failure (loosening) zone.

3 CONCLUSIONS

The mechanism of face failure was visually investigated on a three-dimensional basis in this study through a tunnel pull-out model test using X-ray CT. Also, the volume of the failure zone associated with face failure was evaluated quantitatively. The findings are summarized as follows:

- 1) The mechanism of face failure can be visually investigated nondestructively and three-dimensionally by the test method used in this study.
- 2) A semicircular slip surface is generated behind the face, and the failure zone extends straightly upward with an elliptic cross-sectional shape above the tunnel.
- 3) Arching effect occurs at an overburden of 2D or more. The shape and the volume of the failure zone do not depend much on overburden.
- 4) When a large-scale failure is caused by a pull-out length of 10 mm, a failure zone develops along a slip surface similar to that observed in the critical state.

The authors intend to further study the mechanism of face failure on a three-dimensional basis, with such attempts as load measurements on a face, application of surcharge on a ground model, and use of cohesive soil as a soil material. Eventually, an advanced design method is to be developed by introducing three-dimensional stability analysis based on the mechanism found in this study.

REFERENCES

- Chambon, P. and Cort e, J.F. 1994. Shallow Tunnels in Cohesionless Soil: Stability of Tunnel Face. *J. of Geotech. Eng. Div. ASCE*, 120, 7, 1148-1165.
- Konishi, S., Asakura, T., Tamura, T. and Tsuji, T. 2000. Evaluation of tunnel face stability for sand strata with clay layers. *J. of Geotechnical Engineering, JSCE*, 52, 659, 51-62. (in Japanese).
- Mashimo, H., Suzuki, M. and Inokura, A. 1999. Study on evaluation method of tunnel face stability. *J. of Geotechnical Engineering, JSCE*, 49, 638, 117-129. (in Japanese).
- Otani, J., Mukunoki, T., and Obara, Y. 2000. Application of X-ray CT method for characterization of failure in soils. *Soils and Foundations*, 40, 2, 111-118.
- Otani, J., Mukunoki, T., and Obara, Y. 2002a. Characterization of failure in sand under triaxial compression using an industrial X-ray CT scanner. *Journal of Physical Modelling in Geotechnics*, 1, 15-22.
- Otani, J., Mukunoki, T., and Kikuchi, Y. 2002b. Visualization for engineering property of in-situ light weight soils with air foams. *Soils and Foundations*, 42, 3, 93-105.